



Chiral Liquid Crystal-Based Sensor for the Detection of Low Humidity

Nimet Yilmaz Canli & Zeynep Güven Özdemir

To cite this article: Nimet Yilmaz Canli & Zeynep Güven Özdemir (2015) Chiral Liquid Crystal-Based Sensor for the Detection of Low Humidity, *Molecular Crystals and Liquid Crystals*, 623:1, 64-73, DOI: [10.1080/15421406.2015.1010857](https://doi.org/10.1080/15421406.2015.1010857)

To link to this article: <http://dx.doi.org/10.1080/15421406.2015.1010857>



Published online: 21 Dec 2015.



Submit your article to this journal [↗](#)



Article views: 13



View related articles [↗](#)



View Crossmark data [↗](#)

Chiral Liquid Crystal-Based Sensor for the Detection of Low Humidity

NİMET YILMAZ CANLI* AND ZEYNEP GÜVEN ÖZDEMİR

Department of Physics, Yıldız Technical University, Istanbul, Turkey

The humidity sensing capability of a film of (S)-5-octyloxy-2-[[4-(2-methylbutoxy)-phenylimino]-methyl]-phenol liquid crystal (LC) was studied. The experimental results show that LC thin film offers a promising perspective as a sensing material for the detection of relatively low humidity levels at even room temperature. It was observed that the operating temperature has a considerable effect on humidity sensing performance of the sensor. A comparison of kinetic models applied to the adsorption of water molecules on the LC film was evaluated for the Ritchie and Elovich kinetic models. Linear regression analysis results show that Elovich equation provides the best correlation for the water molecule adsorption processes.

Keywords Chiral liquid crystal; Elovich equation; humidity sensor; response time; sensitivity

1. Introduction

Humidity sensors (HSs), which measure the amount of water vapor present in a gas, have a crucial importance in both industrial processing and environmental control [1]. HSs have been utilized in various fields of industry and life sciences such as semiconductor industry, automobile industry, medical applications, agriculture, textile production, meteorological analysis, forecasting etc. [2, 3]. Various chemoresistive metal oxide sensors have been used to detect humidity, which include Al_2O_3 [4, 5], TiO_2 [6–8], SiO_2 [9]; semiconductors such as SnO_2 [10–12], In_2O_3 [13–16], and polymers [1]. Well-known disadvantages of inorganic semiconductor gas sensors are their low selectivity, high operating temperature, long response and recovery time of the sensor signal [17–19].

Humidity sensors are also usually classified as capacitive or resistive type. Capacitive sensors have a more linear response than the resistive sensors. While capacitive sensors are used for both very low (0%) to high (100%) relative humidity (RH), the resistive type of HSs are typically limited to about 20% to 90% RH. Especially, very low humidity levels have a critical importance on telecommunications. Low levels of humidity can cause brittle circuit boards and greatly increase the buildup of static electricity, which often creates electrical discharge and uncontrollable malfunctions.

In recent years, the chemical sensor applications of liquid crystals (LCs) have been investigated such as detection of cholic acid [20], vaporous butylamine in air [21], heavy

*Address correspondence to Nimet Yilmaz Canli, Department of Physics, Yıldız Technical University, 34210 Istanbul, Turkey. Email: niyilmaz@yildiz.edu.tr

Color versions of one or more of the figures in the article can be found online at www.tandfonline.com/gmcl.

metals in aqueous [22] etc. In this context, we have focused on the research of the effect of humidity of chiral liquid crystal (LC), since there has been no report on the issue of this type of liquid crystal. According to our results, chiral LC ((S)-5-octyloxy-2-[[4-(2-methylbutoxy)-phenylimino]-methyl]-phenol) film offers a promising perspective as sensing material for the detection of (1%–4%) low RH levels at room temperature.

Measuring very low RH has a crucial importance for various kinds of applications such as battery industry, medical device technology, agriculture, biology, etc. As is known, dry rooms at which RH is 1%, are used for lithium battery manufacturing, automotive hybrid batteries, and medical devices. Measuring very low RH has also a significant role in agriculture and biology. For instance, the highest survival rate of entomopathogenic fungi, which has a great potential for using it as a bio-pesticide in agriculture, requires very low relative humidity (<5%) [23, 24]. In this context, the chiral LC material may be utilized as HS to measure extremely very low RH for the advanced technological applications mentioned above.

2. Experimental

The synthesis details of the chiral Liquid Crystalline Compound ((S)-5-octyloxy-2-[[4-(2-methylbutoxy)-phenylimino]-methyl]-phenol) was reported elsewhere [25–28]. The chemical structure of LC is presented in Fig. 1.

Liquid crystal compound was easily dissolved in chloroform in order to obtain 1 mg/mL solution. Prior to the deposition of thin film of LC by spin-coating technique, interdigital array of metal electrodes were patterned on cleaned glass substrate using photolithography. Prior to vacuum evaporation, glass substrates were thoroughly cleaned by ultrasonically

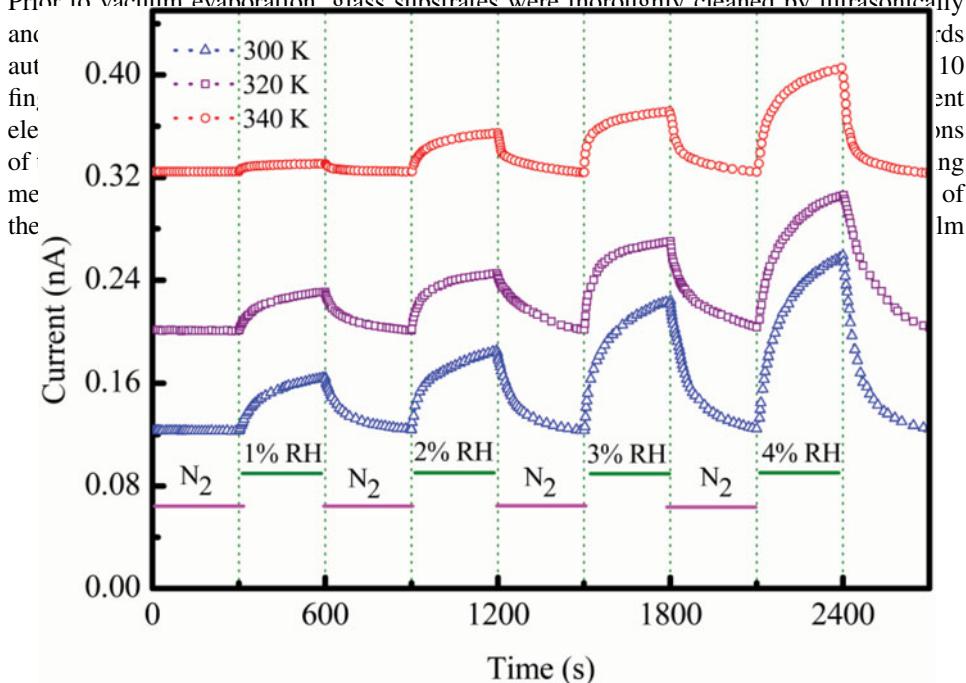


Figure 1. The chemical structure, phase transition temperatures T ($^{\circ}\text{C}$) and transition enthalpies ΔH (kJ mol^{-1}) of the liquid crystal compound (LC).

was measured in a homemade teflon chamber implemented in our laboratory where dry nitrogen gas (N_2) was used as carrier gas. The carrier gas used in the experiments had purity level of 99%. For humidity measurements, the N_2 gas was divided into dry gas and wet gas, which was prepared by bubbling the N_2 gas through deionized water. Then, wet N_2 gas was mixed with dry N_2 gas using computer-derived mass flow controllers (MKS Inst.). The RH inside the measurement chamber was varied between 0% and 10% RH and controlled with a commercially available humidity meter. The variation of the sensor current during sensing experiments was monitored by using a Keithley 6517A electrometer. A dc voltage of 1 V was applied to the sensor during the measurements. A typical experiment consisted of exposure to test gases and subsequent purging with dry nitrogen. Humidity sensing data were recorded by IEEE-488 data acquisition system incorporated to a personnel computer.

3. Results and Discussion

Sensing experiments were performed at different temperatures in order to find out the optimum operating temperature of this film for RH sensing. The response currents of the LC film exposed to different RH, following an increasing RH order of 1%, 2%, 3%, and 4% were recorded. Figure 2 shows the effect of various concentrations of water molecules on the dynamic response of the LC coated interdigital transducer at indicated temperatures. Both adsorption and desorption times were set at 5 min. As can be seen from the Fig. 2, when the film is exposed to various concentration of water vapors, the sensor current increases sharply in the initial doping stage followed by a drift to the steady-state value. It is also clear from Fig. 2 that when the water vapor was turned off, purging with dry nitrogen leads to an initial fast decrease followed by a slow drift until the current reaches its initial value. This proves that the adsorption process is reversible. The sensing performance of the films toward sequential RH pulses can be explained as follows. The first step of the detection of a molecule is the adsorption of the molecule on the surface of the material. When the water molecules adsorbed at the active adsorption sites, it results in charge transfer interaction between the water molecules and surface of the film. This interaction leads to a change in

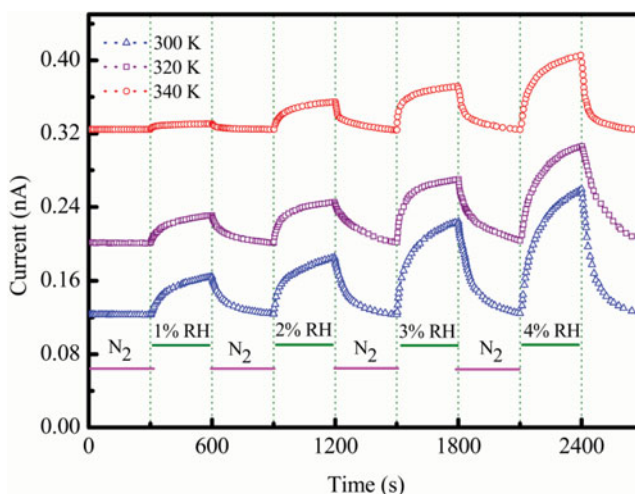


Figure 2. Dynamic response–recovery characteristics of the LC coated sensor to 1%, 2%, 3%, and 4% RH at three different temperatures.

electrical conductivity of the film. The adsorption of a water molecule on the film surface leads to the creation of an acceptor level.

These acceptor states, which lie below the Fermi level at the initial stage of adsorption, make easy the trapping of valance electrons. When the number of the trapped electrons reaches to a sufficient value, the Fermi level shifts towards the valance band. This shift in the Fermi level causes the reduction in the speed of trapping processes. When the sensor is then exposed to dry nitrogen, this leads to desorption of adsorbed water molecules from the surface of the active sensing layer, and thus a decrease in sensor current.

The sensing curves for various temperatures, shown in Fig. 2, look similar to each other and it is hard to compare the sensing characteristics among them since the initial sensor currents are not identical for different temperatures. Such problem is solved by using response (R) instead of sensor current. Figure 3 shows the response, defined by $R = (I_{RH} - I_0)/I_0$ where I_{RH} is the sensor current in the presence of humidity and I_0 is the film current in dry nitrogen gas, as a function of RH at various temperatures. For all temperatures investigated, there is a good linearity between the response magnitude and the level of RH. Examining this graph, it is clear that the response of the sensor decreases as the level of RH increases. The sensitivity of the sensor towards RH was obtained from the slope of the Fig. 2. The response plot in Fig. 2 gives the sensitivity values of $2.55 \times 10^{-1} (\%)^{-1}$ and $1.67 \times 10^{-2} (\%)^{-1}$ at 300 K and 350 K, respectively. It is evident that the sensitivity of the sensor decreases with increasing temperature. Similar results on sensitivities have been reported for some other gases coated with different sensing materials [29].

The interpretation of the decrease in sensitivity as the temperature increases requires taking into account many elementary physico-chemical processes. The temperature dependence of the sensitivity suggests that the temperature either decreases the number of active sites on the surface or complicate the adsorption of water molecules into the existing sites. The observed effect can be attributed to the thermally induced structural changes, at least partly.

To investigate the effect of operating temperature, the response and recovery rate of the film were compared by response and recovery time. The response time τ_{90} is defined

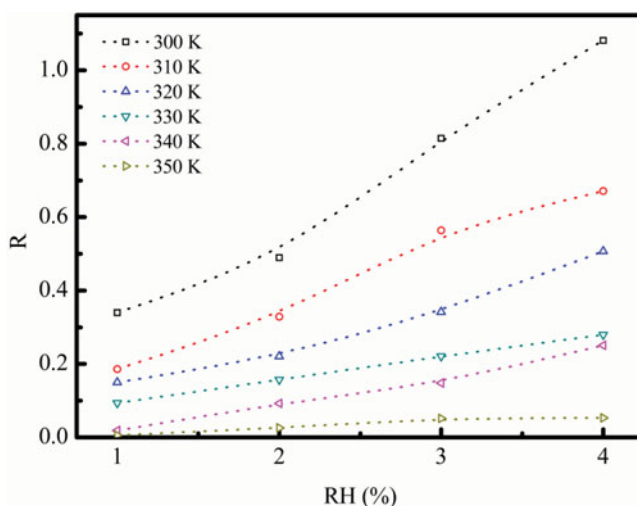


Figure 3. Normalized responses of LC sensor as function of RH at indicated temperatures.

as the time it takes to reach 90% of the final current. The response time τ_{90} were obtained from the measured dynamic response–recovery characteristics (Fig. 3). The derived values of τ_{90} as function of RH level at different operating temperatures are shown in Fig. 4(a). The response time of the sensor for 3% RH was approximately 120 s at room temperature. With increasing temperature, the response time decreases rapidly. At 350 K, its value was 55 s. It is clear from Fig. 4(a) that elevation of operating temperature leads to a smaller value of τ_{90} for the investigated sensor.

The recovery time (τ_{10}), defined as the time required to return to 10% below its equilibrium value in dry N_2 . According to this definition, a small value of the τ_{10} represents a quick recovery to its initial state. The variation of the recovery time with RH is shown in Fig. 4(b). The results also show that the recovery time of the sensor is an increasing function of the RH level, on the other hand, it is a decreasing function of temperature. This observation suggests that by increasing the sensing temperature the recovery characteristic

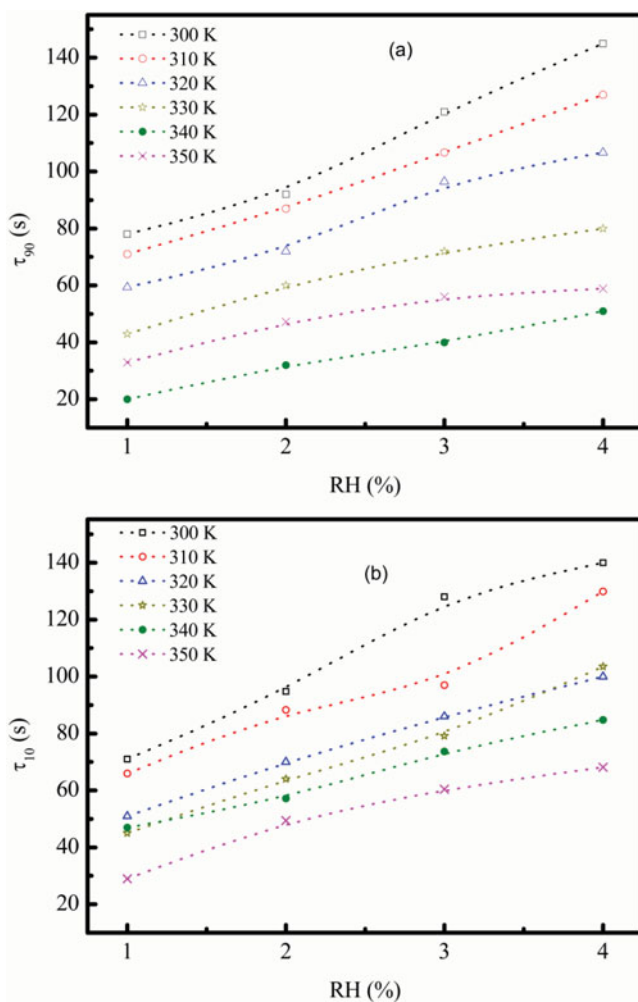


Figure 4. RH dependence of the response time (a) and recovery time (b) at various temperatures for the film of LC.

can be improved. The observed response and recovery behavior of the sensor can be explained by the adsorption–desorption kinetics.

3.1. Kinetic Studies

Most adsorption kinetics processes are usually controlled by different mechanisms, of which the most limiting are the diffusion mechanisms, attributed to rapid external diffusion or boundary layer diffusion and surface adsorption. In order to gain insight into the adsorption process, a suitable kinetic model is needed to analyze the experimental data. In order to investigate the mechanisms of adsorption, numerous kinetic models such as Elovich model and Ritchie's equation have been suggested. In this study, the adsorption of water vapors onto LC film was modeled using these rate equations. The conformity between experimental data and the model predicted values was expressed by the correlation coefficients (R^2). A relatively high R^2 value indicates that the model successfully describes the kinetics of water vapors adsorption onto the LC film surface.

3.2. Ritchie Equation

Ritchie proposed a model for gas–solid adsorption processes [30]. According to Ritchie, the rate of adsorption depends solely on the fraction of sites which are unoccupied at time t , then

$$\frac{d\theta}{dt} = \alpha(1 - \theta)^m \quad (1)$$

where θ is the fraction of surface sites, which are occupied by adsorbed gas, m is the number of surface sites occupied by each molecule of adsorbed gas, and α is the rate constant. By applying the boundary conditions $\theta = 0$ at $t = 0$ and $\theta = q_t/q_e$ at $t = t$, Eq. (2) integrates to

$$\frac{q_e^{m-1}}{(q_e - q_t)^{m-1}} = 1 + (m - 1)\alpha t \quad \text{for } m \neq 1 \quad (2)$$

When introducing the amount of adsorption, q_t , at time t , and if gas adsorption is considered to be a second-order reaction, then Eq. (2) becomes:

$$\frac{1}{q_t} = \frac{1}{\alpha q_e t} + \frac{1}{q_e} \quad (3)$$

Ritchie proposed that the sorption capacity and rate constant α can be calculated from the intercept and the slope of the $1/q_t$ vs. $1/t$ plot.

3.3. Elovich Model

The Elovich equation, which is another rate equation based on the adsorption capacity, was developed to describe the kinetics of chemisorption of a gas onto solids. Elovich equation has been widely used to describe the adsorption of gas onto solid systems and adopted to examine the mechanism of the adsorption process, which is expressed by

$$\frac{dq_t}{dt} = \alpha \exp(-\beta q_t) \quad (4)$$

The parameter α represents the rate of chemisorption at zero coverage and the parameter β is related to the extent of surface coverage and the activation energy of chemisorption and q_t is the quantity of gas adsorbed during the time t [31]. The integrated form of Eq. (4) can be written in the form

$$q_t = \frac{2.3}{b} \log(t + t_0) - \frac{2.3}{b} \log t_0 \quad (5)$$

with

$$t_0 = \frac{1}{ab} \quad (6)$$

To simplify Elovich's equation, Chien and Clayton [32] assumed that $abt \gg 1$ and by applying the boundary conditions $q_t = q_t$ at $t = t$ and $q_t = 0$ at $t = 0$, the integrated form

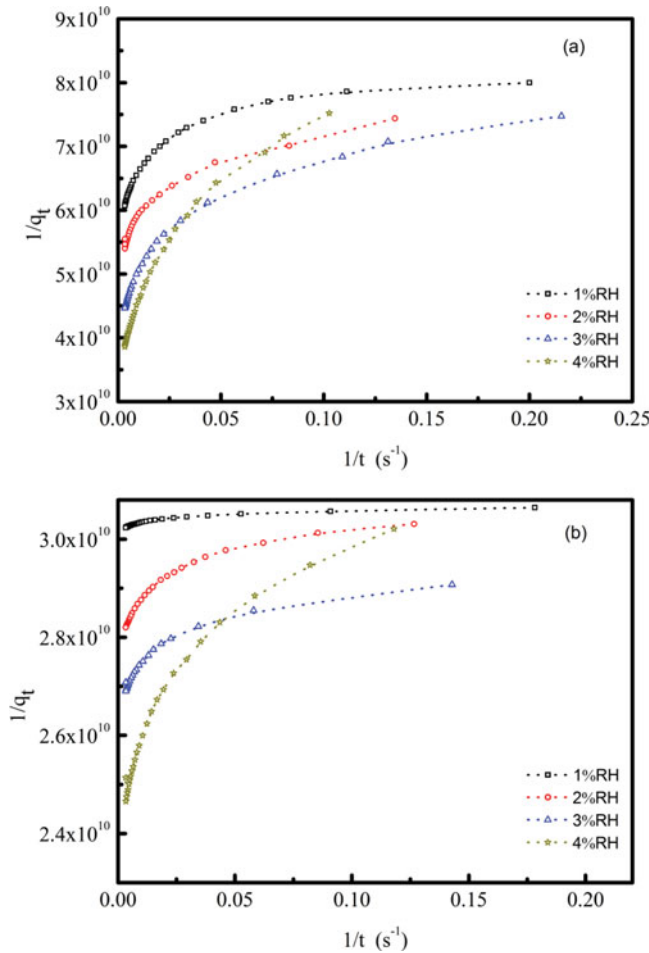


Figure 5. Plot of Ritchie equation for sorption of water molecules onto the LC film (a) at room temperature (b) at 340 K.

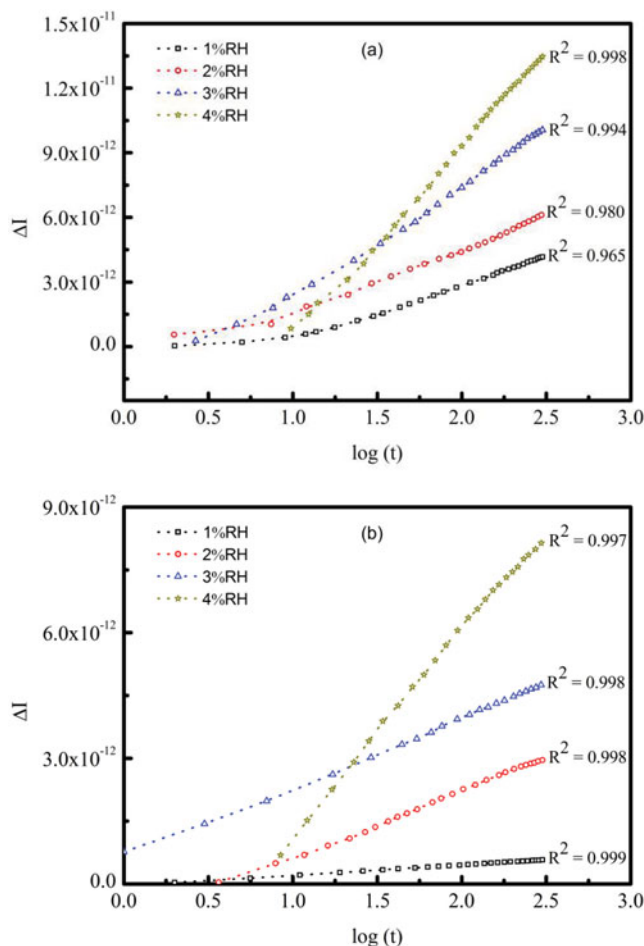


Figure 6. Elovich plots for water molecules adsorption onto the LC film (a) at room temperature (b) at 340 K.

of Eq. (4) becomes,

$$q_t = \frac{1}{b} \ln(ab) + \frac{1}{b} \ln(t) \quad (7)$$

3.4. Test on Kinetics Models

Figure 5(a) and (b) show $(1/q_t)$ vs. $1/t$ plot for various concentrations of water vapors at room temperature and 340 K, respectively. It is important to note that for a Ritchie model, the correlation coefficient is always less than 0.975 for all RH range investigated, which is indicative of a bad correlation. This confirms that Ritchie equation is not appropriate to use as a model to predict the adsorption kinetics of water molecules onto the LC film.

By assuming that the change in the current (ΔI) is proportional to the change in surface coverage, the applicability of Eq. (7) cannot be checked by the plot of ΔI versus $\ln(t)$, a should be a straight line. A set of $\Delta I - \ln(t)$ plots, which are derived from Fig. 2, for room

temperature and 340 K, adsorption of water vapors with various concentrations on LC film surface are shown in Fig. 6(a) and (b), respectively. It reveals that the plots of ΔI versus $\ln(t)$ are linear for all RH levels, indicating that the interaction obeys the Elovich equation.

4. Conclusion

The spin-coating film humidity sensor based on chiral liquid crystal compound ((S)-5-octyloxy-2-[[4-(2-methylbutoxy)-phenylimino]-methyl]-phenol) has been successfully developed. The humidity sensing properties of the film was studied as a function of temperature and RH level. All the observations demonstrated that superior humidity sensing can be achieved by the film of the LC even at room temperature. A comparative study of the applicability of kinetic models of Ritchie and Elovich to describe the adsorption of water molecules on thin film of LC has been carried out. Comparing the regression coefficients R^2 shows that the Elovich model best describes the experimental data on the adsorption of water molecules with studied samples.

Acknowledgments

The authors wish to thank Prof. Dr. Ahmet Altındal for his value discussions on humidity sensor properties. We also would like to thank Prof. Dr. Belkiz Bilgin Eran for her contributions on liquid crystals.

References

- [1] Chen, Z., & Lu, C. (2005). *Sensor Lett.*, 3, 274.
- [2] Traversa, E. (1995). *Sensor Actuat. B*, 23, 135.
- [3] Kolpakov, S. A., Gordon, N. T., Mou, C., & Zhou, K. (2014). *Sensors*, 14, 3986.
- [4] Khanna, V. K., & Nahar, R. K. (1986). *J. Phys. D: Appl. Phys.*, 19, L141.
- [5] Chakraborty, S., Nemoto, K., Hara, K., & Lai, P. T. (1999). *Smart Mater. Structure*, 8, 274.
- [6] Traversa, E., Gnappi, G., Montenero, A., & Gusmano, G. (1996). *Sens. Actuat. B*, 31, 59.
- [7] Wu, R., Sun, Y., & Chen, H. (2004). *Chem. Sens. (Suppl. B)*, 20, 372.
- [8] Grimes, C. A., *et al.* (2000). *J. Appl. Phys.*, 87, 5341.
- [9] Krutovertsev, S. A., Tarasova, A. E., Krutovertseva, L. S., & Zorin, A. V. (1997). *Sensor Actuat. A*, 62, 582.
- [10] Racheva T. M., & Critchlow, G. W. (1997). *Thin Solid Films*, 292, 299.
- [11] Ansari, S. G., Ansari, Z. A., Kadam, M. R., Karekar, R. N., & Aiyer, R. C. (1994). *Sensor Actuat. B*, 21, 159.
- [12] Popova, L. I., Andreev, S. K., Gueorguiev, V. K., & Stoyanov, N. D. (1996). *Sensor Actuat. B*, 37, 1.
- [13] Kleperis, J., *et al.* (1995). *Sensor Actuat. B*, 28, 135.
- [14] Vaivars, G., *et al.* (1996). *Sensor Actuat. B*, 33, 173.
- [15] Tahar, R. B. H., Ban, T., Ohya, Y., & Takahashi, Y. (1998). *J. Am. Ceram. Soc.*, 81, 321.
- [16] Arshak K., & Twomey, K. (2002). *Sensors*, 2, 205.
- [17] Liu X., Cheng S., Liu H., Hu S., Zhang D., & Ning H. (2012). *Sensors (Basel)*, 12, 9635.
- [18] Korotcenkov, G. (2013). *Handbook of Gas Sensor Materials: Properties, Advantages and Shortcomings for Applications Volume 1: Conventional Approaches (Integrated Analytical Systems)*, Springer: New York, USA.
- [19] Zhang, F. X. (1993). *Sensor Application and Its Circuit Selection*, Press of Chinese Electronic Industry: Beijing, PRC.
- [20] He, S., *et al.* (2013). *Anal. Methods*, 5, 4126.
- [21] Ding, X., & Yang, K. L. (2012). *Sensor Actuat. B*, 173, 607.

- [22] Hu, Q. Z., & Yang, C. H. (2011). *Colloids. Surf. B Biointerfaces*, 88, 622.
- [23] Glare, T. R. (2004). In: *Fungal Biotechnology in Agriculture, Food and Environmental Applications*, Arora, D. K., Bridge, P. D., & Bhatnagar, D. (Eds.), Chapter 7, Marcel Dekker Inc: New York, p. 79.
- [24] Moore, D., Douro-Kpindou, O. K., Jenkins, N. E., & Lomer C. J. (1996). *Biocontrol Sci. Technol.*, 6, 51.
- [25] Yilmaz Canli, N., Nesrullajev, A., Yasa, O., & Bilgin Eran, B. (2009). *J. Optoelectron Adv. M.*, 1(3), 577.
- [26] Nesrullajev, A., & Bilgin Eran, B. (2008). *Cryst. Res. Technol.*, 43, 308.
- [27] Bilgin Eran, B., Nesrullajev, A., & Yilmaz Canli, N. (2008). *Mater. Chem. Phys.*, 111, 555.
- [28] Yilmaz Canli, N., *et al.* (2010). *Sol. Energ. Mat. Sol. C.*, 94, 1089.
- [29] Özer, M., Altındal, A., Özkaya, A. R., Bulu, M., & Bekaroğlu, Ö. (2005). *Synthetic Met.*, 155, 222.
- [30] Ritchie, A. G. (1977). *J Chem Soc. Faraday Trans.*, 73, 1650.
- [31] Aharoni, C., & Tompkins, F. C. (1970). In: *Advances in Catalysis and Related Subjects*, Eley, D. D., Pines, P., & Weisz, P. B. (Eds.), Academic Press: New York, p. 1.
- [32] Chien, S. H., & Clayton, W. R. (1980). *Soil Sci. Soc. Am. J.*, 44, 265.